

## Behavior of silicon-, sulfur-, and tellurium-related $DX$ centers in liquid-phase-epitaxy and vapor-phase-epitaxy $GaAs_{1-x}P_x$ alloys

E. Calleja, F. J. Sanchez, E. Muñoz, and E. Vigil\*

*Departamento de Ingeniería Electrónica, Escuela Técnica Superior de Ingenieros de Telecomunicación, Universidad Politécnica, Ciudad Universitaria, 28040 Madrid, Spain*

F. Omnès and P. Gibart

*Centre de la Recherche sur l'Heteroepitaxie et ses Applications, Parc Sophia Antipolis, Avenue Bernard Gregory, 06560 Valbonne, France*

J. M. Martin and G. Gonzalez Díez

*Departamento de Electricidad y Electrónica, Facultad de Ciencias, Universidad Complutense, Ciudad Universitaria, 28040 Madrid, Spain*

(Received 27 November 1995)

Several series of Te-doped  $GaAs_{1-x}P_x$  layers grown by liquid phase epitaxy and vapor phase epitaxy are analyzed by deep-level transient spectroscopy (DLTS), photoluminescence, and thermally stimulated capacitance techniques. In addition to the *well-established* Te- $DX$  center (trap  $A$ ), DLTS spectra reveal two distinct peaks labeled  $B$  and  $C$  in the literature. These two traps, of unknown origin so far, but showing  $DX$ -like fingerprints, are actually donor-related  $DX$  centers generated by Si and S residual contamination. This finding, supported by results in Si- and S-implanted samples, clarifies a long standing question about the origin of these traps and their suggested relation to local environment effects. For the first time, to our knowledge, fingerprints (thermal and optical barriers) of the Si-related  $DX$  centers in  $GaAs_{1-x}P_x$  have been established. A warning is given about the high risk of experimental data misinterpretation in cases where residual contamination is present. A *clear* and *strong* statement about the *existence of Te- $DX$  centers in  $GaAs_{1-x}P_x$  alloys* has to be made against recent published works, to avoid more confusion in the future.

### I. INTRODUCTION

Most of the early research on  $n$ -type  $GaAs_{1-x}P_x$  alloys focused on S- and Te-doped material, grown either by liquid phase epitaxy (LPE) or vapor phase epitaxy (VPE). Early studies on  $DX$  centers in  $GaAs_{1-x}P_x$  related these traps to extended defects and dislocations.<sup>1,2</sup> S- $DX$  centers, characterized by Craford *et al.*<sup>3</sup> and Craven and Finn,<sup>4</sup> have thermal emission and capture barriers of 0.35 and 0.15 eV, respectively.<sup>4</sup> Te- $DX$  centers have thermal emission and capture barriers of 0.17 and 0.06 eV (trap  $A$ ).<sup>5-8</sup> Two more traps have been detected very frequently in this material, depending on the sample and/or epitaxial reactor, with thermal emission energies of 0.27 (trap  $C$ ) and 0.38 eV (trap  $B$ ). Both electron traps have typical  $DX$ -center fingerprints,<sup>5-8</sup> and trap  $C$  was suggested to be a second  $DX$  center related to Te donors because of its concentration scaling to that of trap  $A$ .<sup>6,7</sup> However, the precise origin of traps  $B$  and  $C$  remain unclear to date.

The effects of the local environment on  $DX$  centers, shown by the splitting of the emission deep-level transient spectroscopy (DLTS) signal in Si-doped  $Al_xGa_{1-x}As$ ,<sup>9,10</sup> restored the interest of  $DX$  centers in  $n$ -type  $GaAs_{1-x}P_x$ . Following Chadi's model,<sup>11</sup> Si donors in  $Al_xGa_{1-x}As$  generate one group of four split levels because it is the Si atom that moves along the  $[111]$  direction and senses either Al or Ga atoms as near neighbors. On the other hand, Dobaczewski *et al.*<sup>12</sup> propose that Te donors in  $Al_xGa_{1-x}As$  generate two distinct groups of levels, since the

moving atom may be either Ga or Al. They also suggest the existence of up to four groups of levels in Te-doped  $GaAs_{1-x}P_x$ ,<sup>13</sup> since the ionic barrier for the emission process is now formed by As and P atoms. Then, unlike the case of Si-doped  $Al_xGa_{1-x}As$ , DLTS spectra in Te-doped  $GaAs_{1-x}P_x$  might reveal quite *different emission energies* from various local configurations. Then the presence of traps  $A$ ,  $B$ , and  $C$ , observed by DLTS in Te-doped  $GaAs_{1-x}P_x$ , could be taken as evidence of these local environment effects.

On the other hand, the model that describes electron emission from  $DX$  centers through a two-step process (negative  $U$ ) has never been *directly* corroborated by DLTS or any other technique, to our knowledge, and there is a controversy about the interpretation of recent experimental data formerly taken as evidence of a two-photoionization process.<sup>14,15</sup> The lack of reliable information on the stability of the  $DX^0$  state and its thermal energy makes it difficult to select DLTS experimental conditions (temperature, window ratio, sampling time) to detect it. It is also hard to predict what the signal intensity, expected from this emission, should be. These facts, together with the concentration ratio found between traps  $A$  and  $C$  in Te-doped  $GaAs_{1-x}P_x$ ,<sup>6,7</sup> may lead us to speculate that these two traps are the signature of a two-step thermal emission process.

In this work we demonstrate that the three main electron traps, usually measured by DLTS in Te-doped  $GaAs_{1-x}P_x$  (labeled as traps  $A$ ,  $B$ , and  $C$ ), correspond to the emission process from  $DX$  centers generated by the dominant donor

TABLE I. GaAs<sub>1-x</sub>P<sub>x</sub> samples characteristics.

Sample No.	Growth method	Donor	Doping level (cm <sup>-3</sup> )	% P		Remarks
				Nominal	(PL)	
1	LPE	Te	9.3×10 <sup>17</sup>	35	(31)	
2	LPE	Te	4.0×10 <sup>16</sup>	42	(48)	
3	VPE	Te	9.3×10 <sup>16</sup>	40	(38)	
4	VPE	Te	2.1×10 <sup>17</sup>	40	(41)	
5	VPE	Te	2.0×10 <sup>16</sup>	40	(38)	
6	VPE	Te	8.0×10 <sup>17</sup>	40	(39)	Zn-diffused p <sup>+</sup> -n LED
7	VPE	Te + Si	2.1×10 <sup>17</sup>  5.0×10 <sup>12</sup> a	40	(41)	Former No. 4 with Si implantation
8	VPE	Te + S	2.1×10 <sup>17</sup>  5.0×10 <sup>12</sup> a	40	(41)	Former No. 4 with S implantation
9	MOVPE	Si	1.0×10 <sup>17</sup>	21	(20)	Test sample

<sup>a</sup>Total dose (cm<sup>-2</sup>).

(Te) and to *two other donor species* that are present in the alloy due to contamination during the growth process, namely, Si and S. A significant Si contamination has been found to be very common in Al<sub>x</sub>Ga<sub>1-x</sub>As layers grown by metal-organic vapor phase epitaxy (MOVPE);<sup>16</sup> however, GaAs<sub>1-x</sub>P<sub>x</sub> samples studied in this work were grown either by LPE or standard VPE. These results highlight the above speculations as clear examples of a dramatic misinterpretation when potential residual contamination is not assessed and considered.

## II. EXPERIMENT

GaAs<sub>1-x</sub>P<sub>x</sub> single layers and homojunction light-emitting diodes (LED's) from various manufacturers, grown either by liquid phase epitaxy (LPE) or vapor phase epitaxy (VPE) on *n*-type GaAs substrates, were studied. All compositions were in the range of 35–42 % phosphorous (nominal) and Te doping levels varied from low 10<sup>16</sup> to 1×10<sup>18</sup> at/cm<sup>-3</sup>. Table I lists the samples characteristics. Schottky barriers were deposited on GaAs<sub>1-x</sub>P<sub>x</sub> single layers, whereas LED's had a ring top ohmic contact. The active areas of these devices were different and the absolute values of the capacitance cannot be compared directly. Photoluminescence (PL), constant voltage DLTS, thermally stimulated capacitance (TSCAP), and photocapacitance versus wavelength (*C-W*) measurements were performed. DLTS conditions were the same for all measurements:  $V_f=0.5$  V,  $V_r=-0.5$  V,  $t_f=300$  ms, and  $t_2/t_1=4/2$  ms.

In order to clarify the origin of traps *B* and *C*, two pieces of sample No. 4 (Table I) were implanted with Si<sup>29</sup> and S<sup>32</sup> at 150 and 80 KeV, respectively, with a total dose of 5

×10<sup>12</sup> cm<sup>-2</sup>. A rapid thermal annealing (RTA) process at 875 °C during 10-s activated Si and S donors. Another GaAs<sub>1-x</sub>P<sub>x</sub> (21%) test layer, doped with Si to 1 ×10<sup>17</sup> cm<sup>-3</sup> (sample No. 9) was grown by metal-organic vapor phase epitaxy (MOVPE).

## III. RESULTS AND DISCUSSION

### A. Photoluminescence characterization

PL measurements were first carried out in all samples to precisely determine their alloy compositions. Figure 1 shows

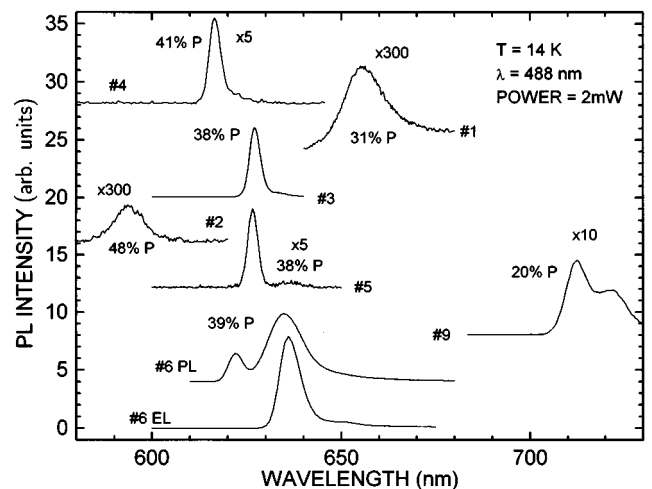


FIG. 1. Photoluminescence and electroluminescence spectra of Te- and Si-doped GaAs<sub>1-x</sub>P<sub>x</sub> samples (see Table I).

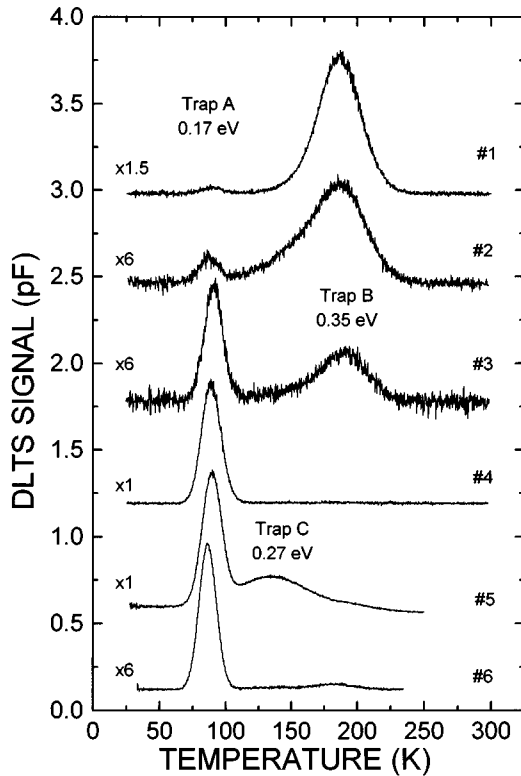


FIG. 2. DLTS spectra of LPE and VPE Te-doped  $\text{GaAs}_{1-x}\text{P}_x$  samples (see Table I).

PL data of some representative Te-doped  $\text{GaAs}_{1-x}\text{P}_x$  samples. All VPE layers exhibit similar compositions and high PL intensities. LPE ones show broader signals with significantly lower intensities, even considering that they are not corrected by the setup response. The actual phosphorus content of sample No. 2 is about 48% (Table I) beyond the crossover, which could partially explain the low PL intensity. However, the broad signals of both LPE samples point to a rather poor crystalline quality. PL and electroluminescence (EL) from sample No. 6, a  $p^+-n$  Zn-diffused LED, reveal transitions involving the Zn acceptor.<sup>17</sup> Sample No. 9, a MOVPE-grown layer, shows a PL spectrum with a transition related to carbon contamination.<sup>17</sup>

### B. DLTS and TSCAP characterization

Figure 2 represents emission DLTS spectra of Te-doped sample Nos. 1–6, either single layers (Schottky) or LED's ( $p^+-n$ ). Te-DX centers are always present (trap A) with an emission energy of 0.17 eV, and a capture barrier of 0.07 eV in VPE samples with 40% P nominal. Trap C has an emission energy of 0.27 eV and a capture barrier of 0.15 eV ( $X=0.38$ ). Both trap fingerprints are in very good agreement with previous results in similar samples.<sup>6</sup> Trap B has an emission energy of 0.35 eV and a capture barrier of 0.15 eV ( $X=0.31$ ), in perfect agreement with the S-DX center fingerprints reported by Craven and Finn.<sup>4</sup> It is important to notice that traps B and C show up depending on the specific sample: trap B is clearly present in sample Nos. 1, 2, and 3, barely seen in sample Nos. 5 and 6, and not detectable in sample No. 4. However, trap C is only seen in sample No. 5 and it is possibly masked by trap B in sample No. 2.

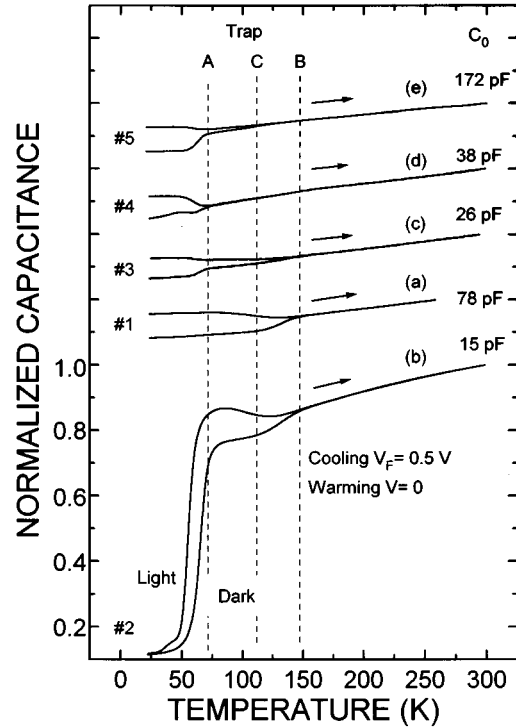


FIG. 3. Normalized TSCAP spectra of LPE and VPE Te-doped  $\text{GaAs}_{1-x}\text{P}_x$  samples in the dark and under light excitation (see text). All spectra were recorded at zero bias. Persistent photocapacitance (PPC) effects due to different traps are present. Total capacitance values at zero bias and 300 K ( $C_0$ ) are given.

Figure 3 shows TSCAP measurements of sample Nos. 1–5 with and without light. Samples were cooled under forward bias of 0.5 V and measured when warming at 0 V. At 20 K the light was turned on for 5 min, then switched off. Light excitation above 1.35 eV ensured the photoionization of Te-DX centers (trap A) (Refs. 4 and 7) and S-DX centers.<sup>3,4</sup> Persistent photocapacitance (PPC) effects are present, and, depending on the sample, TSCAP curves in the dark show steps at different temperatures. The connection points between curves in the dark and after light excitation also appear at different temperatures. We will see below that this is well understood if the number and relative concentration of deep traps present are considered.

A striking result is observed in DLTS spectra of Fig. 2 from the LPE samples (Nos. 1 and 2), namely that trap B is clearly dominant over trap A (Te-DX), although Te is the main donor. TSCAP data provide a clear explanation. Curve a in Fig. 3 (sample No. 1 with  $X=0.31$ ) shows no significant carrier freeze-out and no decay at temperatures below 75 K. This indicates that the Te-DX center is barely occupied, in agreement with the fact that trap A (Te-DX) becomes resonant for  $X \approx 0.30$ .<sup>3,6</sup> It also agrees with a rather small PPC effect. The thermal depth of trap B, expressed as the difference between the emission and capture barriers, is twice as deep as in trap A, which also contributes to its larger DLTS signal. The TSCAP signal decay, starting at 150 K, is due in this case to electron freeze-out in trap B.

However, curve b in Fig. 3 (sample No. 2 with  $X=0.48$ ) first shows a moderate decay at 150 K followed by a strong freeze-out below 75 K. These two “critical” temperatures

are characteristic of electron freeze-out in traps *B* and *A*, respectively. This behavior is expected when considering that the maximum thermal depth for *DX* centers occurs for alloy compositions close to 45% P. Since Te is the main donor, the strong carrier freeze-out produces a dramatic increase of the sample series resistance at temperatures where the DLTS signal of the Te-*DX* shows up. Then the capacitance, as well as the DLTS amplitude, decrease.<sup>18</sup> In addition to this effect, the possibility that the trap *B* concentration is comparable to the main donor one, in the range of  $10^{16}$  cm<sup>-3</sup>, cannot be disregarded.

Finally, in all VPE samples, with compositions close to 40%, the dominant DLTS signal is due to trap *A* (Fig. 2), and there is always a moderate freeze-out below 75 K (Fig. 3). It is worth mentioning that, for sample No. 4, there is only the DLTS signal of Te-*DX* centers, as well as only one step decay of the TSCAP signal at 75 K (curve *d* in Fig. 3). On the other hand, for sample No. 5, there are two DLTS peaks (traps *A* and *C*) as well as two distinct temperatures at which the TSCAP signal decreases (curve *e* in Fig. 3). These results allow us to determine three “critical” temperatures that define the electron freeze-out in traps *A*, *B*, and *C* in alloys with similar compositions. These critical temperatures are related to the capture barrier energies of each trap.

At this point, it should be clarified once again that donors generate different effective-masslike (EM) states linked to each conduction-band (CB) minimum, with thermal depths that depend on the effective-mass values. In the case of GaAs<sub>1-x</sub>P<sub>x</sub>, Al<sub>x</sub>Ga<sub>1-x</sub>As, and other III-V compounds, donors, generate deep states (*DX* centers) whose thermal depths depend strongly on the alloy composition. Then, when the *DX* center is resonant with the CB, its occupation is very small and almost all electrons interact with the shallow, effective-mass-like  $\Gamma$  (or *X*) states. Consequently, small DLTS signals and PPC effects are observed. However, this does not mean that the layer is free from *DX* centers, since a corresponding electronic state does exist: evidence from experiments with hydrostatic pressure is overwhelming. A similar situation arises when the *DX* center presence cannot be ascertained, i.e., by DLTS at low temperature when there is a strong freeze-out (high *DX* center thermal depth). The claim of *DX* center-free layers, often found in the literature, is misleading and it should read “free of *DX* center effects,” since the physical meaning and implications are quite different. This is especially significant in the case of Te-doped GaAs<sub>1-x</sub>P<sub>x</sub>, because there are still authors denying the existence of Te-*DX* centers as deep donor states. This misinterpretation is often due to improper experimental conditions (temperature not low enough), sample selection (the *DX* center is resonant),<sup>3</sup> or just because the Te-*DX* center fingerprints are not properly identified.<sup>19,20</sup> We will come back to this point below.

DLTS emission spectra in Fig. 4 demonstrate that trap *C* is actually the Si-*DX* center in GaAs<sub>1-x</sub>P<sub>x</sub>. Curve *a* from sample No. 4 shows no traces of traps *B* and *C*. Curve *b* from sample No. 5 clearly shows the presence of trap *C*. Curves *c* and *d* correspond to sample No. 7 (former sample No. 4 implanted with Si) and to sample No. 9 (Si doped). This last spectrum was taken under hydrostatic pressure (15 Kbar) to force the Si-*DX* center to merge into the gap, since sample No. 9 has only 20% P. The asymmetry of this peak is thought

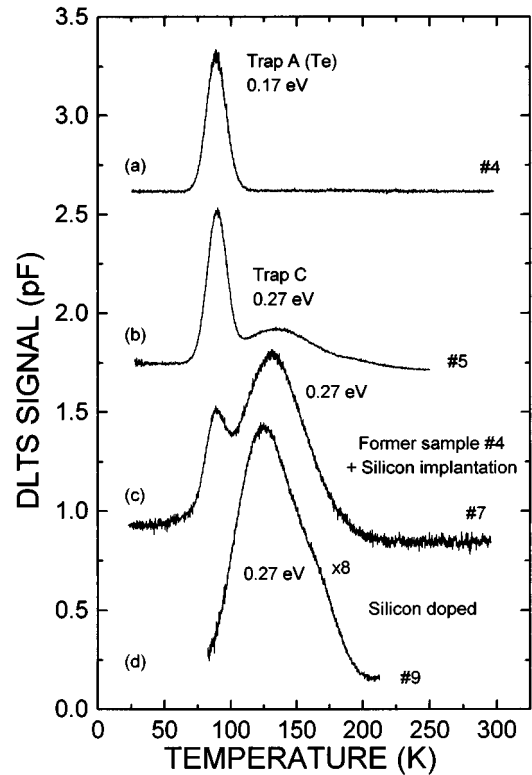


FIG. 4. DLTS spectra of GaAs<sub>1-x</sub>P<sub>x</sub> samples: (curve *a*) Te-doped (No. 4); (curve *b*) Te-doped (No. 5); (curve *c*) Te-doped and Si-implanted (No. 7); and (curve *d*) MOVPE-grown, Si doped (No. 9).

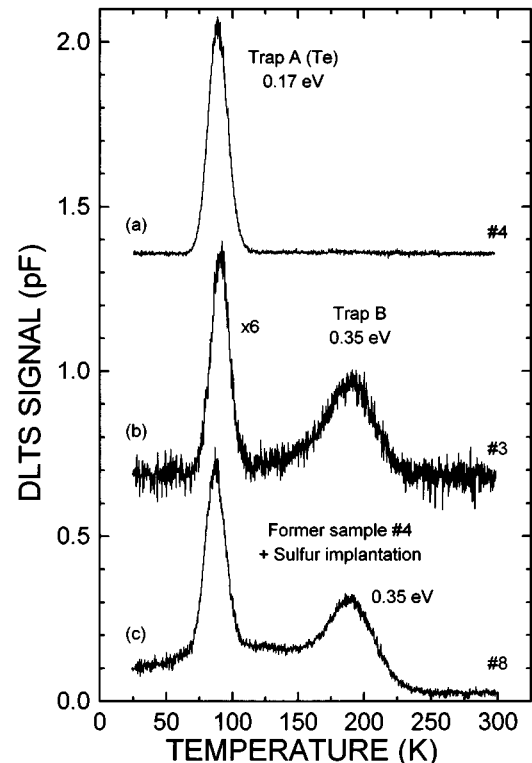


FIG. 5. DLTS spectra of GaAs<sub>1-x</sub>P<sub>x</sub> samples: (curve *a*) Te-doped (No. 4); (curve *b*) Te doped (No. 3); (curve *c*) Te doped and S implanted (No. 8).

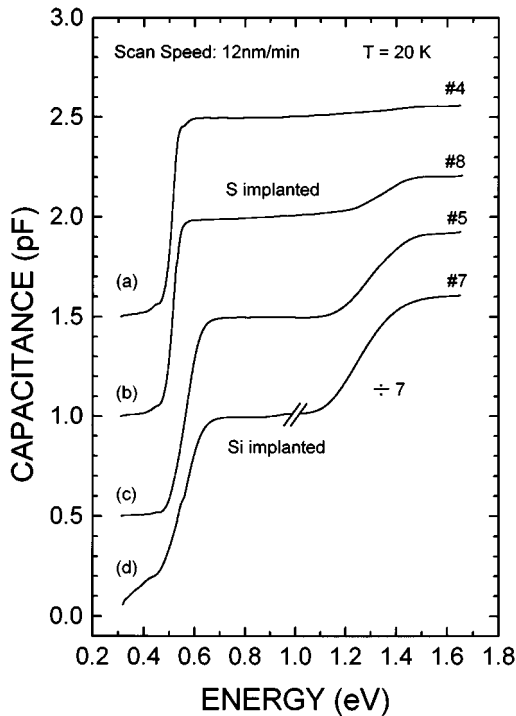


FIG. 6. Photocapacitance spectra of various Te-doped  $\text{GaAs}_{1-x}\text{P}_x$  samples.

to be due to local environmental effects, more pronounced for low-P content. The emission energies and peak temperatures of trap C and the Si-DX center are precisely the same.

Similar conclusions are drawn from data in Fig. 5, where DLTS spectra correspond to *a* the clean sample No. 4; to *b* sample No. 3 where trap B appears; and *c*, to sample No. 8, former sample No. 4 implanted with S. Again, there is a perfect agreement of the emission and capture barriers between trap B and the S-DX center.

### C. Photocapacitance

Figure 6 represents the photoionization spectra of three Te-doped  $\text{GaAs}_{1-x}\text{P}_x$  samples. Curve *a* is obtained from sample No. 4 (clean sample). Curve *b* is from sample No. 8, former No. 4 implanted with sulfur. Curve *c* corresponds to sample No. 5 and reproduces previous results by Calleja *et al.*<sup>7</sup> in commercial red LED's. Curve *d* is measured from sample No. 7, former No. 4 implanted with silicon. All spectra show a sharp photoionization at 0.5–0.6 eV that correspond to the well established threshold of Te-DX centers.<sup>5,7,21</sup> Now, curve *b* reveals the photoionization process of S-DX centers in  $\text{GaAs}_{1-x}\text{P}_x$ , with a threshold energy around 1.2 eV, in agreement with previous results.<sup>3,4</sup> Curves *c* and *d* show the same process for Si-DX centers in  $\text{GaAs}_{1-x}\text{P}_x$  with a threshold energy around 1.05 eV. Notice that these values are not the “exact” threshold energies, because they cannot be derived from a single photocapacitance scan.<sup>22</sup> However, a very slow scan speed was selected so that the error must be quite small. Figure 7 shows in more detail the photoioniza-

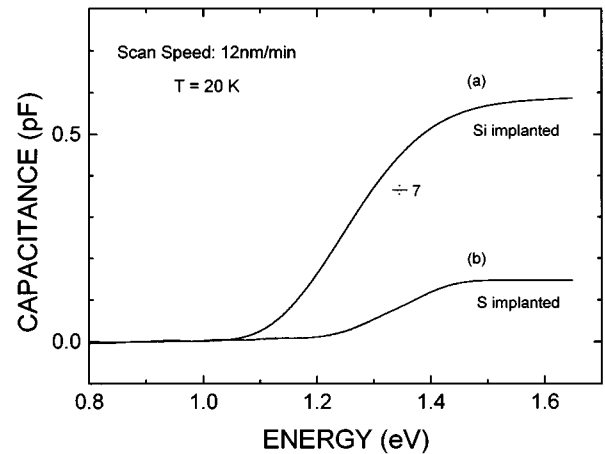


FIG. 7. Photocapacitance spectra of  $\text{GaAs}_{1-x}\text{P}_x$  samples Nos. 7 and 8. In both cases the flat region of spectrum *a* in Fig. 6 (“clean” sample) has been subtracted. Differences in photoionization energies between Si- and S-DX centers are shown.

tion threshold differences between Si- and S-DX centers, obtained by subtracting the flat region of spectrum *a* from spectra *b* and *d* in Fig. 6.

## IV. CONCLUSIONS

These results provide additional evidence about the fingerprints of the Si- and S-DX centers in  $\text{GaAs}_{1-x}\text{P}_x$ , and clarify the origin of the main electron traps in Te-doped  $\text{GaAs}_{1-x}\text{P}_x$ . More specifically, the photoionization threshold energy and the thermal emission and capture barriers for Si-DX centers in  $\text{GaAs}_{1-x}\text{P}_x$  have been established for the first time, to our knowledge. There is also clear evidence of contamination in  $\text{GaAs}_{1-x}\text{P}_x$  grown by LPE and VPE, that might also be present in MOVPE material. Most important, contamination in  $\text{GaAs}_{1-x}\text{P}_x$  and  $\text{Al}_x\text{Ga}_{1-x}\text{As}$  (Ref. 16) might lead to strong misinterpretation of experimental data when establishing the microscopic structure of complex defects, like DX centers. A clear example is shown in Fig. 7, where the photoionization process of Si- and S-DX centers coincide at a given photon energy with quite different optical cross sections. Then photoionization transients in a device containing both donor species, even present with a high concentration ratio, would be nonexponential, no matter the technique used to minimize other intrinsic sources of nonexponentiality.<sup>23</sup> These results could erroneously be taken as proof of a two-step photoionization process.

Emphasis must be placed on correcting a recurrent misinterpretation about a long-established fact: Te-DX centers do exist in Te-doped  $\text{GaAs}_{1-x}\text{P}_x$ . Two examples must be considered: a recent work from Li *et al.*<sup>19</sup> in 1994, and a work from Kaminski<sup>20</sup> in 1993. In the first case, Te-DX centers are not recognized in Te-doped  $\text{GaAs}_{1-x}\text{P}_x$  with 40% P, although the DLTS fingerprints<sup>6</sup> are clearly measured in their work (LT peak in Fig. 1.b) The authors attribute this peak to residual implantation-induced defects, arguing that its shape is dependent on the annealing conditions. We have shown here that silicon contamination in VPE samples generates DX

centers with DLTS peaks at temperatures between the ones corresponding to Te- and S-DX centers. Any change of the annealing conditions can modify the relative amplitude of the existing DX centers. In their experiment, a DLTS spectrum of the Te-doped layer, prior to sulfur implantation, should be needed. We also show that 75 K is a critical temperature for Te-DX centers in GaAs<sub>1-x</sub>P<sub>x</sub> 40% P, where thermal capture and emission coexist; emission being a much slower process due to its larger activation energy (Fig. 3).

On the other hand, the work by Kaminski reveals a rough confusion when ascribing the origin of different traps found in Te-doped VPE GaAs<sub>1-x</sub>P<sub>x</sub> 40% P. Trap T1 is said to be either a Te-DX center or a Te<sub>As</sub>Ga<sub>As</sub>Te<sub>As</sub> complex. Trap T2 is identified as a O<sub>i</sub>Te<sub>As</sub> complex. Trap T3 would be a point defect involving a group-V vacancy, dependent on the dislocation density. Finally, trap T4 is claimed to be a point defect involving a group-V antisite. In summary, a complete family

of complex defects, but neither traces of the ubiquitous Te-DX center as a simple substitutional donor nor references to previous works where the presence of these Te-DX centers have been undoubtedly demonstrated. Let us suggest a much simpler explanation: traps T1, T2, and T4 are Te-DX centers. T1 and T2 differ in temperature position and amplitude, when the charge pulse is changed, due to local environment effects.<sup>9,21,23,24</sup> Trap T3 is just the sulfur-related DX center.

#### ACKNOWLEDGMENTS

We want to acknowledge the technical assistance of F. Gonzalez-Sanz and J. Sánchez for device processing, and G. Nataf and J. M. Sallese for the growth of GaAs<sub>1-x</sub>P<sub>x</sub> by MOVPE. This work was partially supported by CICYT Project Nos. TIC-930025 and TIC-930026.

\*Permanent address: Fac. de Ciencias, IMRE, Universidad de La Habana, La Habana-Vedado, Cuba.

<sup>1</sup>L. Forbes, *Solid-State Electron.* **18**, 635 (1975).

<sup>2</sup>G. Ferenczi, in *New Developments in Semiconductor Physics*, edited by F. Beleznyay, G. Ferenczi, and J. Gibber (Springer-Verlag, Berlin, 1980), Vol. 122, p. 176.

<sup>3</sup>M. G. Craford, G. E. Stillman, J. A. Rossi, and N. Holonyak, *Phys. Rev.* **168**, 867 (1968); *J. Electron. Mater.* **20**, 3 (1991).

<sup>4</sup>R. A. Craven and D. Finn, *J. Appl. Phys.* **50**, 6334 (1979).

<sup>5</sup>I. D. Henning and H. Thomas, *Solid-State Electron.* **25**, 325 (1982).

<sup>6</sup>E. Calleja, E. Muñoz, and F. García, *Appl. Phys. Lett.* **42**, 528 (1983).

<sup>7</sup>E. Calleja, E. Muñoz, B. Jiménez, A. Gomez, F. García, and F. Kellert, *J. Appl. Phys.* **57**, 5295 (1985).

<sup>8</sup>M. Kaniewska and J. Kaniewski, *J. Appl. Phys.* **63**, 1086 (1988).

<sup>9</sup>E. Calleja, A. Gomez, J. Criado, and E. Muñoz, in *Defects in Semiconductors*, edited by G. Ferenczi, Materials Science Forum Vols. 38–41 (Trans. Tech., Aedermansdorf, Switzerland, 1989), p. 1115.

<sup>10</sup>E. Calleja, F. García, A. Gomez, E. Muñoz, P. M. Mooney, T. N. Morgan, and S. L. Wright, *Appl. Phys. Lett.* **56**, 934 (1990).

<sup>11</sup>D. J. Chadi and K. J. Chang, *Phys. Rev. Lett.* **61**, 873 (1988); *Phys. Rev. B* **39**, 10 063 (1989).

<sup>12</sup>L. Dobaczewski, P. Kaczor, M. Missous, A. R. Peaker, and Z. R. Zytkeiwicz, *Phys. Rev. Lett.* **68**, 2508 (1992).

<sup>13</sup>L. Dobaczewski, P. Kaczor, M. Missous, A. R. Peaker, and Z. R. Zytkeiwicz, *J. Appl. Phys.* **78**, 2468 (1995).

<sup>14</sup>L. Dobaczewski and P. Kaczor, *Phys. Rev. Lett.* **66**, 68 (1991).

<sup>15</sup>Z. Su, J. W. Farmer, and M. Mizuta, *Phys. Rev. B* **48**, 4412 (1993).

<sup>16</sup>E. Calleja, F. Sanchez, E. Muñoz, P. Gibart, A. Powell, and J. S. Roberts, *J. Electron. Mater.* **24**, 1017 (1995).

<sup>17</sup>A. G. Milnes, in *Deep Impurities in Semiconductors* (Wiley, New York, 1973).

<sup>18</sup>A. Broniatowski, A. Blossie, P. C. Srivastava, and J. C. Bourgoin, *J. Appl. Phys.* **54**, 2907 (1983). See also A. L. Romero, A. Calleja, F. García, E. Muñoz, A. L. Powell, P. I. Rockett, R. Grey, and P. A. Claxton, *Appl. Phys. Lett.* **61**, 1811 (1992).

<sup>19</sup>M. F. Li, Y. Y. Luo, P. Y. Yu, E. R. Weber, H. Fujioka, A. Y. Du, S. J. Chua, and Y. T. Lim, *22nd International Conference on the Physics of Semiconductors, Vancouver, Canada, 1994*, edited by D. J. Lockwood (World Scientific, Singapore, 1995), Vol. 3, p. 2303.

<sup>20</sup>P. Kaminski, *Semicond. Sci. Technol.* **8**, 538 (1993).

<sup>21</sup>E. Calleja and E. Muñoz, in *Physics of DX Centers in GaAs Alloys*, edited by J. C. Bourgoin, *Solid State Phenomena* Vol. 10 (Sci-Tech, Vaduz, Liechtenstein, 1989), pp. 73–98.

<sup>22</sup>R. Okumura and T. Ikoma, *Appl. Phys. Lett.* **25**, 572 (1974).

<sup>23</sup>E. Calleja and I. Izpura, in *DX Center Donors in AlGaAs and Related Compounds*, edited by E. Muñoz, *Defect and Diffusion Forum* Vol. 108 (Scitech, Untermuhleweg, Switzerland, 1994), Chap. 4, and references therein.

<sup>24</sup>J. M. Sallese, D. K. Maude, M. L. Fille, U. Willke, P. Gibart, and J. C. Portal, *Semicond. Sci. Technol.* **7**, 1245 (1992).